2017 21st International Conference on Process Control (PC)
June 6–9, 2017, Štrbské Pleso, Slovakia

Position Control of Servo Drive With a State Observer

Igor Bélai and Mikuláš Huba
Faculty of Electrical Engineering and IT
Slovak University of Technology in Bratislava
Bratislava, Slovakia
Email: igor.belai@stuba.sk, mikulas.huba@stuba.sk

***Abstract*—The paper is dedicated to the design and comparison of a positional servo drive with two alternative control structures. PD controller and a state observer are used in two model based control approaches, which differ in type of the state observer. One of them contains an inverse plant model combined with filters of the position and velocity feedback (DO-FPID control). Their orders are optional. The second structure includes an extended state observer (ESO) combined again with filters in the position and velocity feedback. However, the filter orders are not optional and follow from the ESO structure (ESO-PID control). In addition, in both structures a setpoint feedforward is utilized. Its purpose is to minimize the control error during continuous position reference changes. Tuning of the controller, state observer and feedforward parameters are presented in the paper. Properties of the considered position controllers are verified through simulation.**

I. Introduction

The speed servo drive control using a disturbance observer (DO), a PD controller and a position signal filtration has been explored in several papers [1]-[5]. They proposed tuning of the controller and binomial filters used both in the DO and the stabilizing feedback. For the sake of simplicity, the same nth order filter may be required. This is enabled by an appropriate feedforward design [4], [5].

In active disturbance rejection control (ADRC) [6] - [8] the essential element is represented by an extended state observer (ESO). ESO can be implemented by using linear functions only, or they can be combined with some nonlinear terms. One can then talk about linear or nonlinear ESO. The manipulated variable and the output from the sensor of a main controlled variable are fed to the inputs of ESO. The observed output variable, its first derivative and the input disturbance represent the ESO outputs. The feedforward output is added to the output of the controller and it directly affects the manipulated variable in DO-FPID control. In the ADRC, the feedforward is implemented by a transient profile generator and its output represents the reference for the first derivative of the main controlled variable. The chosen ESO type affects the structure of the controller and in case of nonlinear ESO, the nonlinear functions used in the observer are applied in the controller, too [6], [7]. The linear PD controller may be used in combination with a linear ESO [8].

The presented control structure uses a linear ESO to estimate the position, the angular velocity and the load torque. The transient profile generator performs a feedforward. This feedforward utilizes the first and higher derivatives of the reference position. It allows to minimize the control deviation regardless of the setpoint waveform. The ESO parameters are set to its maximum dynamics. Tuning of a linear PD controller is done in a control loop with neglected ESO dynamics, whereby the pole placement method is applied.

The paper is structured as follows. In Chapter II. the plant to be controlled is described. Chapter III. brings performance measures used for the loop optimization. Control structures considered are described in Chapter IV. An in-depth analysis and controller tuning is focused on the extended state observer (ESO) structure. PD controller tuning and a feedforward control design described in Chapter V. may be combined with both the DO and the ESO. Simulation results presented in Chapter VI. demonstrate performance of particular solutions. They are yet compared with the traditional cascaded P-PI control and summarized in Conclusions.

II. Controlled system

The controlled system contains a torque generator and a mechanical drive subsystem. The torque generator is modeled by a dead time T_a and the mechanical drive subsystem is modeled by a 2nd order plant model with the parameters a_1 and a_0, corresponding to a moment of inertia and to a viscous friction coefficient. The torque generator may be realized by DC or AC drive using appropriate control. The paper does not deal with methods of creating the torque generator. The input disturbance d_i is equivalent to a load torque and it is added to the output of controller u_r representing the torque reference. The output y of the controlled system is in (1). Transfer functions of the actuator $F_a(s)$ and of the plant $S_2(s)$ are in (2) and (3).

$$Y(s) = \left(U_r(s)F_a(s) + D_i(s)\right) S_2(s) \tag{1}$$

$$F_a(s) = e^{-T_a s} \tag{2}$$

$$S_2(s) = \frac{Y(s)}{U_a(s)} = \frac{1}{s(a_1 s + a_0)} \tag{3}$$

III. Evaluation of the control performance

Nearly monotonic transients may represent the optimal closed loop response to the setpoint change [2]. This response may be denoted as a 0P output. The input u_r of the controlled

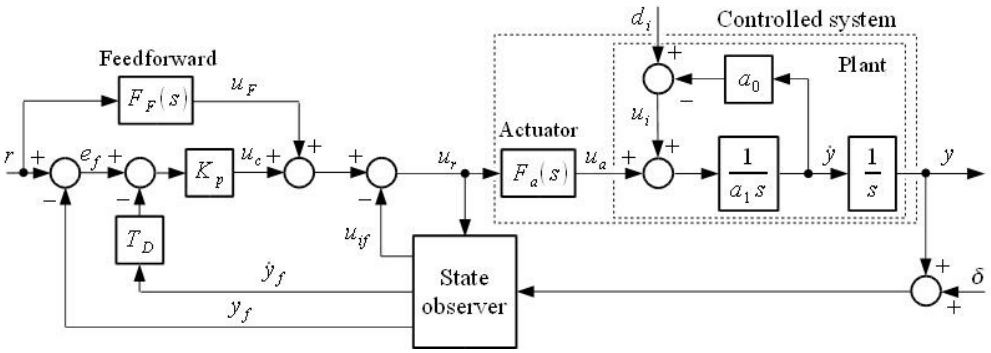

Fig. 1. A general structure of the control loop, δ - quantization noise

system has to lead to "two pulses" and will be denoted as a 2P input. An ideal response to disturbance d_i step can be characterized by "one pulse" shape and will be denoted as a 1P output. To evaluate the deviations from the ideal waveforms with the extreme points u_{m1}, u_{m2}, the integral measures (4)–(6) were introduced in [2]. These are based on Total Variance index given in [9].

$$TV_0(y) = \sum_i |y_{i+1} - y_i| - |y_\infty - y_0| \quad (4)$$

$$TV_1(\dot{y}) = \sum_i |\dot{y}_{i+1} - \dot{y}_i| - |2\dot{y}_{m1} - \dot{y}_\infty - \dot{y}_0| \quad (5)$$

$$TV_2(u) = \sum_i |u_{i+1} - u_i| - |2u_{m1} - 2u_{m2} - u_\infty - u_0| \quad (6)$$

Because the response is supposed to be without any overshoot then the speed of transients at the plant output may be quantified by the IAE (Integral of Absolute Error) [1], [2], [3], [9]:

$$IAE = \int_0^\infty |e(t)|\, dt; e(t) = r(t) - y(t) \quad (7)$$

IV. Considered control structures

A general structure of the control loop is in Fig. 1. The structure of the controlled plant corresponds to (1)-(3), where the block *Actuator* is the torque generator. The PD controller output is described by (8), where K_p and T_D are the gain and the derivative time constant, $Y_f(s)$ and $\dot{Y}_f(s)$ are Laplace transforms of the observed plant output and its derivative.

$$U_c(s) = K_p \left[R(s) - Y_f(s) - \dot{Y}_f(s) T_D) \right] \quad (8)$$

The feedforward $F_F(s)$ should eliminate the error e, so that $e = r - y \to 0$.

At the output of the *State observer*,a filtered total input disturbance u_{if} is observed. Two types of state observers are represented by the *State observer* block: the disturbance observer (DO) combined with filters of the speed and position feedback and the linear extended state (and disturbance) observer (ESO) including an implicit filtration. The structures of state observers are in Fig. 2 and Fig. 3.

The transfer function of the plant model $S_M(s) = 1/(a_1 s^2)$ is utilized in disturbance observer (DO) in Fig. 2. The filters $Q_n(s)$ attenuate the quantization noise δ. The n-th order filters are applied, but in the process of deriving the formulas to

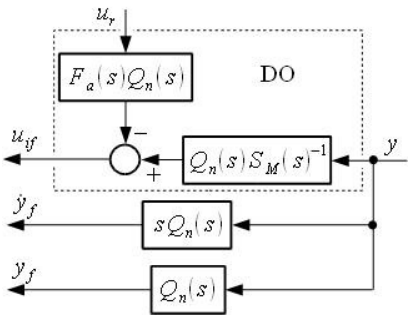

Fig. 2. The structure of the state observer with a disturbance observer (DO) and with the filtered feedback signals

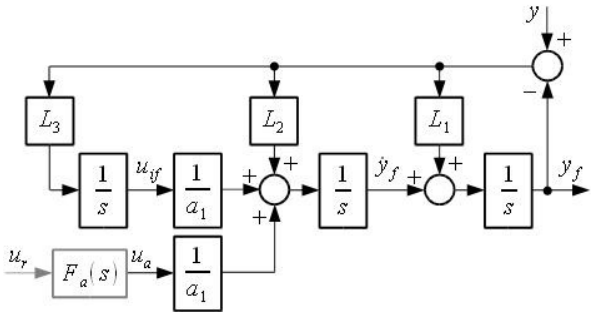

Fig. 3. The structure of the extended state observer (ESO)

calculate the parameters, the filters are replaced by a dead time T_d according to (9) and (10).

$$Q_n(s) = \frac{1}{(T_n s + 1)^n} \approx e^{-T_d s}; n = 2, 3, ... \quad (9)$$

$$T_d = nT_n \quad (10)$$

A. Linear extended state observer

Based on the plant model (6) and real output angular position from the controlled system, the linear ESO (see Fig. 3)

is constructed as [7]

$$\begin{aligned}\frac{dz_1}{dt} &= z_2 + L_1\,(y - z_1)\\ \frac{dz_2}{dt} &= \frac{z_3}{a_1} + \frac{u_a}{a_1} + L_2\,(y - z_1)\\ \frac{dz_3}{dt} &= L_3\,(y - z_1)\end{aligned} \tag{11}$$

$$z_1 = y_f; z_2 = \dot{y}_f; z_3 = u_{if} \tag{12}$$

where $\mathbf{L} = [L_1, L_2, L_3]$ is the observer gain vector.

B. Tuning of linear ESO

The Laplace forms of vector $\mathbf{z}$ components, may be expressed as functions of u_a, y:

$$\begin{aligned}Z_1(s) &= F_o(s)\,(Y(s)F_{1a}s + U_a(s)F_{1b}s)\\ Z_2(s) &= F_o(s)\,(Y(s)F_{2a}s + U_a(s)F_{2b}s)\\ Z_3(s) &= F_o(s)\,(Y(s)F_{3a}s - U_a(s))\end{aligned} \tag{13}$$

where

$$\begin{aligned}F_{1a}(s) &= s^2\frac{a_1L_1}{L_3} + s\frac{a_1L_2}{L_3} + 1\\ F_{1b}(s) &= s\frac{1}{L_3}\\ F_{2a}(s) &= s^2\frac{a_1L_2}{L_3} + s\\ F_{2b}(s) &= s^2\frac{1}{L_3} + s\frac{L_1}{L_3}\\ F_{3a}(s) &= s^2a_1\\ F_o(s) &= \frac{L_3/a_1}{s^3 + s^2L_1 + sL_2 + L_3/a_1}\end{aligned} \tag{14}$$

If the transfer function $F_o(s)$ has a triple real pole $-\omega_{ESO}$, then the gains of observer may be calculated by (15).

$$L_1 = 3\omega_{ESO}; L_2 = 3\omega_{ESO}^2; L_3 = a_1\omega_{ESO}^3 \tag{15}$$

The value of ω_{ESO} may be expressed as function of sampling period T_s

$$\omega_{ESO} = \frac{1}{k_{ESO}T_s} \tag{16}$$

and then for the components of vector $\mathbf{L}$ applies

$$L_1 = \frac{3}{k_{ESO}T_s}; L_2 = \frac{3}{k_{ESO}^2T_s^2}; L_3 = \frac{a_1}{k_{ESO}^3T_s^3} \tag{17}$$

V. Tuning of the controllers

The controller parameters for both controls and the time constants of filters $Q_n(s)$ in DO-FPID control were designed by the pole placement method. The design is based on the simplified transfer functions $Y(s)/R(s)$. The simplification is based on: 1. The substitution of the filters Q_n by an equivalent dead time T_d for DO-FPID control. 2. Ideal state observer for ESO-PID control, i.e. $u_{if} = u_i$, $\dot{y}_f = \dot{y}$, $y_f = y$. 3. The feedforward is not applied.

The second substitution is applied to the transfer functions then. All time delays are substituted by the first order plant transfer functions, as is in (18).

$$e^{-Ts} \approx \frac{1}{Ts + 1} \tag{18}$$

The result are the third order transfer functions $F_{r,DO-FPID}(s)$, $F_{r,ESO-PID}(s)$

$$F_{r,DO-FPID}(s) = \frac{Y(s)}{R(s)} \approx \frac{1}{(T_0s + 1)^3} \tag{19}$$

$$F_{r,ESO-PID}(s) = \frac{Y(s)}{R(s)} \approx \frac{1}{(kT_0s + 1)(T_0s + 1)^2} \tag{20}$$

The parameters of the controller (K_p, T_D) and time delay T_d of the feedback filters Q_n may be expressed from equivalences (19)-(20), where the value of T_0 is optional and it determines the dynamics of the loop. The positions of real poles $-1/T_0$ and $-1/(kT_0)$ are given by the values of calculated parameters.

If the control error does not change its sign, the IAE values corresponding to unit input steps may be derived from simplified transfer function $F_r(s)$ representing the transfer functions $F_{r,DO-FPID}(s)$ or $F_{r,ESO-PID}(s)$.

$$IAE_r = \lim_{s\to 0}\left(\frac{1}{s}\,(1 - F_r(s))\right) \tag{21}$$

The required dynamics of the loop, i.e. the value of T_0 may be derived from the required IAE_r values denoted as IAE_r^*. Thus, T_0 can be derived from (21).

The feedforward transfer function is designed to eliminate the error $e = r - y = 0$. It may be derived from the transfer function $E(s)/R(s)$ by requiring $E(s) = 0$.

A. Tuning with DO

Tuning of controller parameters and feedforward for DO-FPID control is in [4]. Therefore, just the resulting formulas are presented below in (22)-(26).

The value of T_0 is calculated from the required value of IAE_r

$$T_{0,r} = \frac{IAE_r^*}{3} \tag{22}$$

Dead time of the filters Q_n

$$T_d = \frac{a_1T_0}{3a_1 - a_0T_0} - T_a \tag{23}$$

The gain and the derivative time constant of PD controller

$$K_p = \frac{a_1^2}{T_0^2\,(3a_1 - a_0T_0)} \tag{24}$$

$$T_D = 3T_0 \tag{25}$$

The feedforward transfer function

$$\begin{aligned}F_F(s) &= s^3a_1T_a + s^2\,(a_1 + a_0T_a) + sa_0 +\\ &\quad Q_n(s)K_pT_Ds\end{aligned} \tag{26}$$

B. Tuning with ESO

The simplified transfer function $Y(s)/R(s)$ for ESO-PID control is in (27)

$$F_{r,ESO-PID} = \frac{K_p}{s^3 a_1 T_a + s^2 a_1 + s K_p T_D + K_p} \tag{27}$$

The parameters of the controller (K_p, T_D) and the shift of the third real pole $-1/(kT_0)$ may be calculated as

$$k = \frac{T_a}{T_0 - 2T_a} \tag{28}$$

$$K_p = \frac{a_1}{T_0^2(1+2k)} \tag{29}$$

$$T_D = T_0(2+k) \tag{30}$$

The conditions $k > 0$, $K_p > 0$ imply the bottom limitation of T_0:

$$T_0 > 2T_a \tag{31}$$

The IAE value for setpoint step is

$$IAE_{r,ESO-PID} = T_D = T_0 \frac{2T_0 - 3T_a}{T_0 - 2T_a} \tag{32}$$

T_0 guaranteeing the required value of IAE_r may be derived from (32)

$$T_{0,r} = \frac{1}{4}\left(IAE_r^* + 3T_a + \sqrt{(IAE_r^* + 3T_a)^2 - 16 T_a IAE_r^*}\right) \tag{33}$$

The feedforward transfer function is derived from the transfer function $E(s)/R(s) = 1 - Y(s)/R(s)$ which includes the ESO transfer functions (13), (14)

$$\frac{E(s)}{R(s)} = 1 - \frac{(K_p + F_F(s))F_a(s)S_2(s)}{1 + N_{1,ESO}(s) + N_{2,ESO}(s)} \tag{34}$$

where

$$\begin{aligned} N_{1,ESO}(s) &= \left(F_{1b}(s)K_p + F_{2b}(s)K_p T_D - 1\right) F_o(s)F_a(s) \\ N_{2,ESO}(s) &= \left(F_{1a}(s)K_p + F_{2a}(s)T_D K_p + F_{3a}(s)\right) \\ &\quad F_o(s)F_a(s)S_2(s) \end{aligned} \tag{35}$$

The feedforward transfer function and its coefficients are derived from a requirement of $E(s) = 0$. If the transfer function of the actuator $e^{-T_a s}$ is replaced by the transfer function of the first order plant $1/(1+T_a s)$, then the feedforward transfer function $F_F(s)$ in (36), guarantees a zero control error for continuous setpoint signal r.

$$F_F(s) = F_o(s)\left(s^6 k_6 + s^5 k_5 + s^4 k_4 + s^3 k_3 + s^2 k_2 + s k_1\right) \tag{36}$$

TABLE I
DO-FPID CONTROL – THE SETPOINT AND DISTURBANCE STEPS

n	$IAE_r 10^3$	$IAE_i 10^3$	$TV_{2r}(u)$	$TV_{2i}(u)$	$\Sigma TV_2(u)$
2	6.0115	0.3843	5.3795	3.8973	9.2767
3	6.0112	0.3836	2.2185	1.6423	3.8609
4	6.0103	0.3811	1.3086	1.2973	2.6060
5	6.0101	0.3799	1.1843	1.1498	2.3340
6	6.0101	0.3824	1.0076	1.1559	2.1634

where

$$\begin{aligned} k_1 &= K_p T_D \\ k_2 &= \frac{K_p}{L_3}(a_0 + a_1 L_2 T_D + a_0 L_1 T_D) + \frac{a_1 a_0 L_2}{L_3} + \\ &\quad a_1 + a_0 T_a \\ k_3 &= \frac{a_1 L_2}{L_3}(a_1 + a_0 T_a) + \frac{a_1 a_0 L_1}{L_3} + \\ &\quad \frac{K_p T_D}{L_3}(a_1 L_1 + a_0) + a_1 T_a \\ k_4 &= \frac{a_1}{L_3}\left(a_1(L_1 + L_2 T_a) + a_0(L_1 T_a + 1) + K_p T_D\right) \\ k_5 &= \frac{a_1}{L_3}\left(a_1(1 + L_1 T_a) + a_0 T_a\right) \\ k_6 &= \frac{a_1^2 T_a}{L_3} \end{aligned}$$

VI. ILLUSTRATIVE EXAMPLE

To verify the properties of the above mentioned control structures, the MATLAB based simulation model has been used. The interactive model of position servo drive described in [5] was a starting point. Several control structures, including P-PI and DO-FPID structures, are implemented in the model. To verify the properties of the ESO-PID structure, the model has been supplemented by an ESO based position control. The parameters of DC motor HSM 150 with a current control circuit having a torque generator function were used in a simulated drive. To simulate the operation of the incremental rotary encoder (IRC), the actual rotor position has been quantized by $\Delta\varphi$. The parameters of simulated drive:
$a_1 \equiv J = 0.00012$ [kg.m^2]; moment of inertia,
$a_0 \equiv B = 0.00016$ [Nm.s.rad^{-1}]; viscous friction coefficient,
$T_{GM} = 1$ [ms]; torque generator time constant,
$\Delta\varphi = 0.0006283$ [rad]; position sensor resolution,
$T_s = 0.25$ [ms]; sampling period of the controllers.

All internal delays were approximated by the dead time $T_a = T_{GM} + T_s = 0.5$ [ms]. The parameters of controllers were calculated for the IAE_r reference: $IAE_r^* = 0.02$. Parameter values in the model of the drive are the same as they are in the observer.

The position reference signal φ^* was changed stepwise from 0 to 0.3 [rad], or continuously from 0 to 1 [rad]. There was a load torque step change (T_L, i.e. input disturbance d_i) from 0 to 0.1 [Nm] applied at the time $t = 0.5$ [s].

The properties of the position control with the DO-FPID and ESO-PID control are summarized in Tab. I and Tab. II. The feedback filters attenuate the noise in the reference torque signal. This effect relates to both control structures. The values

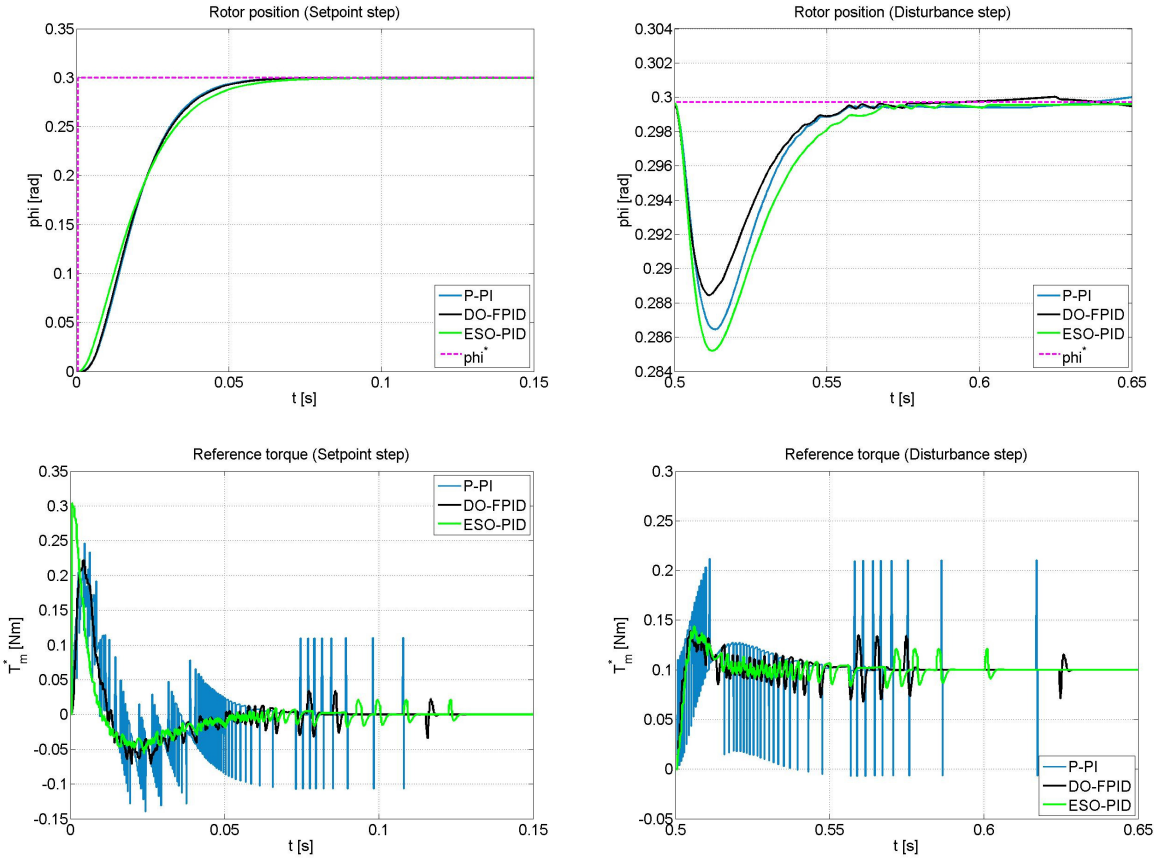

Fig. 4. Transient responses of P-PI, DO-FPID and ESO-PID control ($n = 5$, $k_{ESO} = 4$, $phi \equiv \varphi$, $phi^* \equiv \varphi^*$)

TABLE II
ESO-PID CONTROL – THE SETPOINT AND DISTURBANCE STEPS

k_{ESO}	$IAE_r 10^3$	$IAE_i 10^3$	$TV_{2r}(u)$	$TV_{2i}(u)$	$\Sigma TV_2(u)$
2	5.9637	0.2208	6.7446	3.6343	10.379
3	5.9654	0.3080	2.6237	1.7718	4.3955
4	5.9632	0.4104	1.3393	1.0115	2.3507
5	5.9659	0.5137	0.7932	0.7007	1.4939
6	5.9629	0.6248	0.5214	0.4492	0.9706

TABLE III
P-PI CONTROL – THE SETPOINT AND DISTURBANCE STEPS

$IAE_r 10^3$	$IAE_i 10^3$	$TV_{2r}(u)$	$TV_{2i}(u)$	$\Sigma TV_2(u)$
5.9701	0.3432	16.252	11.023	27.275

of $\Sigma TV_2(u) = TV_{2r}(u) + TV_{2i}(u)$ in the simulation results presented in Tab. I and Tab. II show that the degree of noise attenuation in the reference torque signal is proportional to the order of the filters in the DO-FPID control and also to the position of the triple real pole $-\omega_{ESO} = -1/(k_{ESO}T_s)$ in the extended state observer. Increasing the both, the order of filters in DO-FPID control and the value of k_{ESO} in ESO-PID control, causes a noise reduction in the reference torque signal. However, while the order of the filters has a minimal effect on the value of IAE_i in DO-FPID control, the change of ω_{ESO} significantly affects the size of IAE_i in ESO-PID control.

For comparison, Tab. III shows performance measures for the cascaded P-PI control without a DO and stabilizing feedback filtration according to [4]. The controllers have been tuned to yield a required IAE_r value. Significantly increased $TV_2(u)$ indicates much more grievous noise impact.

Fig. 4 illustrates responses of the output φ and the reference torque T_m^* corresponding to a load step T_L. Obviously, for a step of the reference setpoint φ^*, all responses are nearly equivalent. Responses of the reference torque confirm the fact that the disturbance observer based solutions yield transients with significantly lower torque ripple than the P-PI control. This does not include a low-pass position filter and the quantization noise $\delta = \Delta\varphi$ proceeds to the controller's output without attenuation. The ability to track a continuous position reference is shown in Tab. IV and Fig. 5. The DO-FPID control exhibits the smallest IAE_r value. Therefore, one can conclude that it has the best ability to track the reference position.

VII. CONCLUSIONS

Tuning of a control structure combining ESO with PD control represents the main paper contribution. It is based on prescribing a required IAE value corresponding to unit

TABLE IV
ESO-PID VS DO-FPID VS P-PI CONTROL, CONTINUOUS SETPOINT.
$\varphi^* = 1[rad]$, $k_{ESO} = 4$, $n = 5$.

Control	$IAE_r 10^{-3}$	$TV_{2,r}(u)$
ESO-PID	0.1402	1.8719
DO-FPID	0.0887	1.6078
P-PI	0.1188	39.557

setpoint step. By simulation, the achieved performance has been compared with a DO-FPID and a cascaded P-PI control. Presented control structures with a state and disturbance observer are characterized by a reduction in the signal-to-noise ratio of the desired torque in contrast to P-PI control structure. The two alternatives can be tuned to achieve almost the same speed of responses to the step changes of both the reference position and of the load torque (see the values of IAE_r, IAE_i when $n = 5$ in the Tab. I and $k_{ESO} = 4$ in Tab. II). Slightly lower noise level in the signal of the reference torque has been achieved by use of the DO-FPID control. However, it should be noted that this is true just if the filter order $n = 5$ and $\omega_{ESO} = 1/(4T_s)$. From the response of angular position φ to continuous setpoint changes with an activated feedforward it is obvious that the DO-FPID control allows more accurate reference position tracking. However, the ESO-PID structure is easier to implement, since it contains three integrators and one third order filter in the feedforward. In contrast to this, the equivalent DO-FPID control contains five higher order filters.

Simulations aiming at testing effects of a variable inertia moment on performance of the position control have been carried out, too. Their results (not included in this paper) showed that the DO-FPID control with the fifth order filters is more sensitive than the ESO-PID control.

ACKNOWLEDGMENT

This work has been supported by the grants KEGA 011STU-4/2015 Electronic educational-experimental laboratories of Mechatronics and APVV-0343-12 Computer aided robust nonlinear control design.

REFERENCES

[1] M. Huba and I. Bélai, "Noise attenuation motivated controller design. Part II: Position control," in Speedam Symposium, Capri, Italy, 2014.
[2] M. Huba and I. Bélai, "Experimental evaluation of a DO-FPID controller with different filtering properties," in IFAC World Congress, Cape Town, South Africa, 2014.
[3] M. Huba and I. Bélai, "Comparison of two approaches to a positional servo control," in 15th International Carpathian Control Conference (ICCC 2014), Velké Karlovice, Czech Republic, 2014.
[4] I. Bélai and M. Huba, "The positional servo drive with the feedforward control and the noise attenuation," in Cybernetics & Informatics (K&I 2016), Levoča, Slovakia, 2016.
[5] I. Bélai and M. Huba, "Matlab Based Interactive Model of a Position Servo Drive," in 11th IFAC Symposium on Advances in Control Education (ACE 2016), Bratislava, Slovakia, 2016.
[6] J. Han, "From PID to Active Disturbance Rejection Control," IEEE Transactions on Industrial Electronics, vol. 56, no. 3, March 2009, pp. 900-906
[7] D. Wu, K. Chen and X. Wang "Tracking control and active disturbance rejection with application to noncircular machining," International Journal of Machine Tools & Manufacture, vol. 47, no. 15, Dec. 2007, pp. 2207-2217.

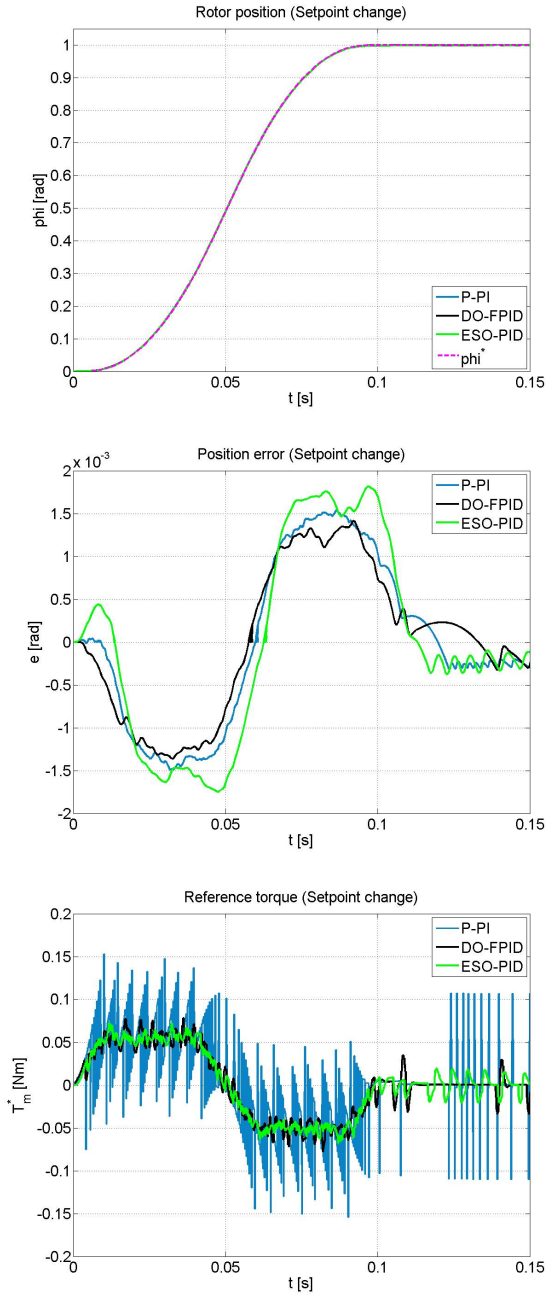

Fig. 5. The responses of P-PI, DO-FPID and ESO-PID control to the continuous reference position ($n = 5$, $k_{ESO} = 4$, $jerk^*$ = 50000 [rad/s^3], $phi \equiv \varphi$, $phi^* \equiv \varphi^*$)

[8] X.H. Yang, X.J. Yang and J.G. Jiang, "A Novel Position Control of PMSM Based on Active Disturbance Rejection," WSEAS Transactions on Systems, vol. 9, no. 11, pp. 1120-1129, 2010.
[9] S. Skogestad, "Simple analytic rules for model reduction and PID controller tuning," Journal of Process Control, vol. 13,, no. 4, pp. 291-309, 2003
[10] S. Triaška, M. Žalman and V. Melich, "Analyses of Air Friction Effect on the Motion System Control," in Technical Computing Bratislava 2012, Bratislava, Slovakia, 2012